journal

J. Am. Ceram. Soc., 74 [10] 2564-72 (1991)

Model of Transformation Toughening in Brittle Materials

I-Wei Chen*

Department of Materials Science and Engineering, University of Michigan, Ann Arbor, Michigan 48109-2136

Assuming that the energy dissipation decreases inversely with distance from the crack tip, the increase in steady-state toughness of a transformation-toughened ceramic is estimated to be $\Delta J = (\Delta J_o/\omega) \ln (1 + \omega)$, where (i) ΔJ_o denotes the toughness increment which would be expected for a given zone height h_o assuming full transformation throughout the zone, and (ii) ω is a nondimensional parameter giving the ratio of the inelastic transformation strain (for full transformation) to the initial elastic strain at the onset of transformation. This estimate extends the earlier result of McMeeking and Evans (1982) in two significant respects: (i) the transformation strain may include a shear component, instead of being purely dilatational, and (ii) the range of ω is now unrestricted, whereas the McMeeking and Evans approach strictly applies only in the weak transformation limit, $\omega << 1$. The height of the inner zone h_i within which transformation has proceeded to completion (or saturation) is estimated to be $h_i = h_o/(1 + \omega)$. Experimental data of Mg-PSZ and Ce-TZP can be quantitatively accounted for using this approximate model, which is also in very good agreement with the rigorous finite-element results of Budiansky, Hutchinson, and Lambropoulos in the special case of subcritical dilatational transformation. [Key words: transformation, fracture toughness, plasticity, zirconia, model.]

I. Introduction

The toughness of certain ceramics can be increased, sometimes by an order of magnitude, by transformation plasticity at the crack tip.[1] In zirconia-containing ceramics, the transformable entity is either a dispersed phase embedded in an inert matrix, such as in magnesia-partially-stabilized zirconia (Mg-PSZ)[1] and zirconia-toughened alumina (ZTA),[2] or the matrix itself, such as in ceria-doped tetragonal zirconia polycrystals (Ce-TZP).[3] In crystallographic terms, the transformation is from a metastable tetragonal symmetry to a stable monoclinic symmetry, and involves a dilatational strain of about 4% and a shear strain of about 16%.[4] When the transformation is triggered by a crack-tip stress field, energy is consumed through the mechanical work that couples the stress and the transformation strain,[5] even though the transformation itself liberates energy. An increase in the work of fracture is a natural consequence of the process.

This toughening effect can be modeled in two ways. In the first approach, the stress-shielding effect at the crack tip due to the residual strain fields which develop following transformation is computed using linear elastic fracture mechanics. This method was initially proposed by McMeeking and Evans.[6] Although their original model takes into account only the dilational part of the transformation strain, assumed to be uniform within the transformation zone, the method is rigorous and can be extended to allow for shear component and partial transformation.[7,8] To do this accurately, however, the model requires a detailed knowledge of strain distribution in the frontal and wake zones surrounding a growing crack. For ceramics, unfortunately, any experimental measurement of crack-tip strains in plane strain fracture seems exceedingly difficult to obtain; thus, a self-consistent method for the determination of these strains needs to be devised in the model. The second approach is to directly estimate the energy dissipation due to transformation that occurs as the crack advances. This energy dissipation, in general, consists of contributions from residual strains in the wake, plastic work expended near the crack tip, and the energy of free surfaces created by the crack-tip stresses. Budiansky, Hutchinson, and Lambropolous[5] have performed these calculations rigorously for a series of dilatationally transforming materials with different strain hardening or softening. Further comparison of these two approaches has been made by Marshall *et al.*[9] and most comprehensively by Rose.[10] In the present work, we attempt to extend the second approach to shear dilatant transformation, using an approximation proposed by Evans, Ahmad, Gilbert, and Beaumont.[11]

A main motivation of our effort is to take advantage of the experimental knowledge of the continuum stress–strain curves of Mg-PSZ and Ce-TZP. Chen and co-workers[12-15] have described these data using a Mohr–Coulomb type of yield criterion that contains two stress invariants, i.e., the hydrostatic stress and the deviatoric stress. They found that the dilatation and the deviatoric components of the transformation strains approximately satisfy the so-called normality condition consistent with the yield criterion.[16] Based on these observations and the theory of classical plasticity, [17,18] a complete set of multiaxial stress–strain relations can be formulated accordingly.[19] It is then feasible to rigorously determine the crack-tip fields of transformation-toughened materials if certain assumptions on unloading paths are made. In principle, therefore, the energy dissipation during crack growth in a shear-dilatant material can be computed.

The rigorous execution of the above procedure in analytic form is extremely difficult because of the mathematical complexity of the crack-growth problems.[20-24] (Rigorous analytic solution for the crack-growth problem is only known for a very few cases.) For this reason, we have adopted the approximate method proposed by Evans, Ahmad, Gilbert, and Beaumont[11] for a similar problem of quantifying toughening enhancement due to rubber dilatation in polymers. In this method, the asymptotic stress–strain field at the tip of a *stationary* crack (the so-called Hutchinson–Rice–Rosengren (HRR) field[25-27]) is used to evaluate the plastic work expended in the crack-tip process zone during loading. If we further ignore the contribution from residual elastic strains in the wake, and assume that the energy of free surfaces created by the crack-tip stresses is the same as in untoughened ceramics, then the toughness increment can be approximately estimated. This approach is taken in the present work.

As preliminaries, we have recently performed elastic–plastic finite-element analysis of the stationary crack-tip field using the above shear-dilatant stress–strain relations. These

A. G. Evans—contributing editor

Manuscript No. 197380. Received July 20, 1990; approved June 20, 1991.
Supported by the National Science Foundation under Grant No. DMR-8807024.
*Member, American Ceramic Society.

results,[28] to be reported elsewhere, confirm the existence of an HRR-type of singular field near the crack tip. With the appropriate stress–strain relations, these results also reproduced the plastic zones similar in shape to the ones observed in Mg-PSZ[8] and Ce-TZP.[29] These findings have provided us some confidence in the constitutive laws adopted.

As a guide to the various cases discussed in our analysis, we introduce the following classification of transformation plasticity. A transformation can be considered as dilatational or shear-dilatant depending on the dominant nature of transformation strain.[12] It can be distinguished as supercritical or subcritical depending on the extent of strain softening or hardening.[5] Lastly, it can be differentiated as weak or strong depending on the relative magnitude of yield strain and transformation strain in the stress–strain curve.[5,30] The major new findings of the present work are concerned with strong, subcritical, and shear-dilatant transformations.

II. Constitutive Relations

The constitutive relations for transformable ceramics were first formulated by Budiansky, Hutchinson, and Lambropoulos.[5] Their model pertains to dilatational transformation only. The case of shear-dilatant transformations[12–13,19] is reviewed below for later reference. The material is assumed to be isotropic at all stages of deformation and its stress–strain behavior is assumed to follow a power law. The normality flow rule is obeyed. The symbols σ and ε are used to denote stress and strain, respectively.

(1) Dilatational Transformation

This case is reviewed first for comparison. The deformation is assumed to be dilatational only and is dictated by the mean stress

$$\sigma_m = \text{mean stress} = \sigma_{kk}/3 \tag{1}$$

If a power law is assumed for the stress–strain curve, we can write

$$\varepsilon_m = \varepsilon_o(\sigma_m/\sigma_o)^n \tag{2}$$

where

$$\varepsilon_m = \text{dilatational strain} = \varepsilon_{kk} \tag{3}$$

and the other symbols are material constants. Without loss of generality, we may let

$$\varepsilon_o = \sigma_o/B \tag{4}$$

where B can be designated as the bulk modulus. In this way, we may identify σ_o with the yield stress and ε_o the yield strain, both in dilatation.

(2) Shear-Dilatant Transformation

We define a generalized effective shear stress (τ_e) as

$$\tau_e = \tau + \mu\sigma_m \tag{5}$$

where

$$\tau = \text{effective shear stress} = \sqrt{(\sigma_{ij} - \sigma_m\delta_{ij})(\sigma_{ij} - \sigma_m\delta_{ij})/2} \tag{6}$$

In Eq. (5), the material constant μ measures the pressure sensitivity of yielding. The stress–strain relation is expressed as

$$\gamma_e = \gamma_o(\tau_e/\tau_o)^n \tag{7}$$

where

$$\gamma_e = \text{effective shear strain} = \sqrt{2(\varepsilon_{ij} - \varepsilon_m/3)(\varepsilon_{ij} - \varepsilon_m/3)} \tag{8}$$

and the undefined symbols are again material constants. This is essentially a Mohr–Coulomb type of yielding generalized for the case of strain hardening. Without loss of generality, we may let

$$\gamma_o = \tau_o/G \tag{9}$$

with G designated as the shear modulus. In this way, we may identify τ_o with the yield stress and γ_o the yield strain, both in shear.

To obey the normality condition, dilatational and shear strains must satisfy

$$\varepsilon_m = \mu\gamma_e \tag{10}$$

The corresponding relation for the yield stresses in pure dilatation, σ_o, and pure shear, τ_o, can be obtained by referring to Eq. (5):

$$\sigma_o = \tau_o/\mu \tag{11}$$

The complete relations between multiaxial stresses and strains were obtained elsewhere[17] and are omitted here.

Values of μ for zirconia-containing ceramics are determined from their yield loci, shown in Fig. 1 for Mg-PSZ and Fig. 2 for Ce-TZP. The intercept of the yield locus with the σ_m axis is σ_o, while the intercept with the τ axis is τ_o. The

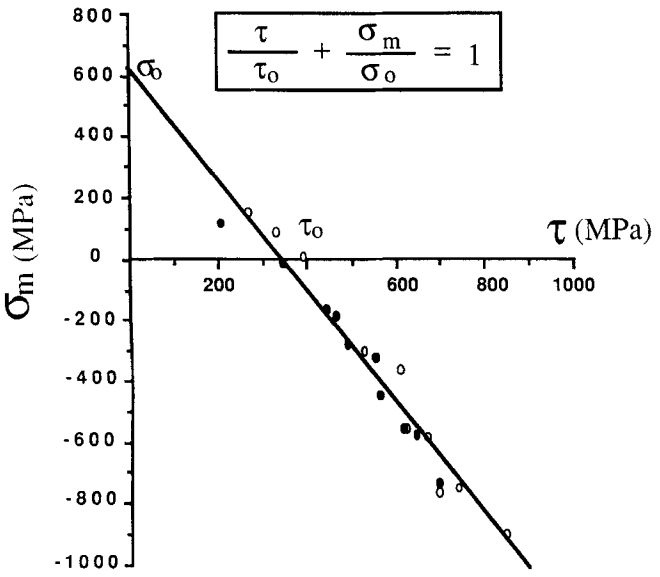

Fig. 1. Yield locus of a Mg-PSZ fitted to a linear shear-dilatant yield criterion.

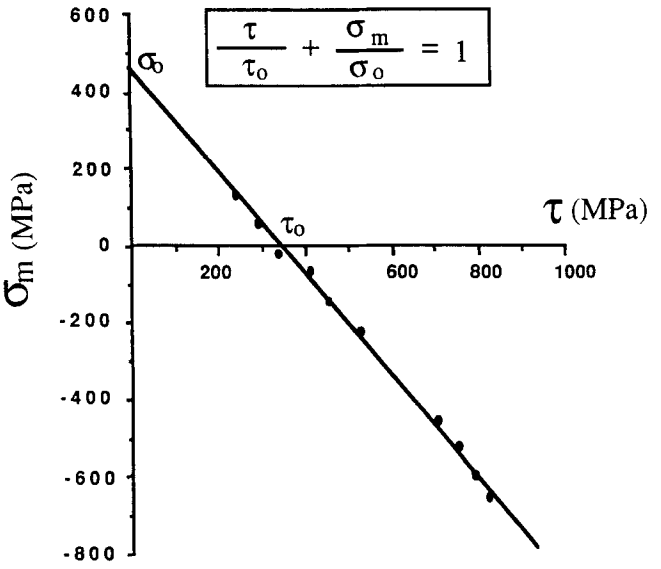

Fig. 2. Yield locus of a Ce-TZP fitted to a linear shear-dilatant yield criterion.

reciprocal slope then is $-\mu$. Experimental methods for obtaining these data are described elsewhere.[12,13,31] From Figs. 1 and 2, we find that $\mu = 0.55$ for Mg-PSZ and $\mu = 0.77$ for Ce-TZP. These values are considerably higher than the ratio computed using Eq. (10) if crystallographic strains ($\varepsilon_m = 0.04$ and $\gamma_c = 0.16$) are adopted, which would have given $\mu = 0.25$. (This implies that approximately 58% (Mg-PSZ) to 68% (Ce-TZP) of the crystallographic shear has been neutralized, by self-accommodation, during transformation under an external stress.) Both μ and yield stresses should be regarded as materials properties dependent on composition and microstructure.

(3) Stress–Strain Curves

The stress–strain curves in compression, with a superimposed hydrostatic pressure, are shown in Fig. 3 for Mg-PSZ and in Fig. 4 for Ce-TZP to illustrate some general features of transformation plasticity.[31] Experimental methods for obtaining these data are described elsewhere.[12,13,31] Both dilatational and shear strain are present and the strain hardening is dependent on the material and test condition. McMeeking and Evans[6] were the first who envisioned a stress–strain curve of a shape similar to the ones shown here. Their stress–strain curve, schematically redrawn in Fig. 5 for dilatational transformation, consists of three stages. The first stage is linear elastic, without transformation. The second stage is relatively flat with a characteristic stress at which transformation proceeds. The third stage is again elastic, with transformation strains exhausted. The experimentally observed stress–strain curves, Figs. 3 and 4, can be similarly interpreted. In particular, the third stage may be approximated as linear elastic having the same elastic modulus as that of the untransformed material; i.e., the slope of the third stage is idealized as the same as the first stage. To make contact with the constitutive relations introduced previously, we also "smooth out" the initial linear elastic portion and the middle plastic portion, and fit them by a single power-law relation. When the stress–strain curves of Figs. 3 and 4 are represented in this way, we find a typical value for n in Mg-PSZ of about 10, while that for Ce-TZP essentially is infinity.

In the above representation, the strains in the constitutive relations refer to total strains, including elastic contributions. Straining below ε_o and γ_o is thus elastic. A limiting strain can be defined by referring to the end of the second stage in Fig. 5, ε_m^*, which is related to the permanent transformation strain, ε_m^T, by

$$\varepsilon_m^T = \varepsilon_m^* - \varepsilon_o \tag{12}$$

A similar definition applies for shear-dilatant transformation:

$$\gamma_c^T = \gamma_c^* - \gamma_o \tag{13}$$

Because of Eq. (10), we may relate these strains by

$$\varepsilon_m^T = \mu\gamma_c^T \tag{14}$$

Referring to these limiting strains, Budiansky *et al.*[5,30] have introduced a dimensionless constant to indicate the strength of transformation. This constant is expressed as the ratio of limiting transformation strain to yield strain, i.e.,

$$\omega_m = \varepsilon_m^T/\varepsilon_o = B\varepsilon_m^T/\sigma_o \tag{15}$$

in dilatational transformation, and

$$\omega_c = \gamma_c^T/\gamma_o = G\gamma_c^T/\tau_o = (G/B)\omega_m/\mu^2 \tag{16}$$

in shear-dilatant transformation. The case of weak transformation corresponds to $\omega_{m,c} << 1$. Conversely, the case of strong transformation corresponds to $\omega_{m,c} >> 1$.

Although the values of saturation strains are sensitive to the microstructure and the driving force, and must be regarded as materials constants, ε_m^T can be directly measured by analyzing the phase content on the fracture surface. Then, with the aid of Eq. (14), γ_c^T can be determined.

(4) Plastic Work

We now establish the formal analogy between the mechanics of dilatational transformation and that of shear-dilatant transformation for the applications sought later. In addition to the constitutive relations formulated above, the plastic work in these transformations, during proportional loading, is examined. (The assumption of proportional loading is valid for a stationary crack but not for a growing crack.) Referring to Fig. 5, the maximum plastic work dissipated by transformation plasticity, when the limiting transformation strain is reached, is shown as the shaded area under the stress–strain curve. Dissipation attains a maximum in this case. In the next section, dissipation of this type will be considered as the source of toughness.

The dissipation energy density, U, over a proportional loading path can be computed by

$$U = \int \sigma_m \, d\varepsilon_m \tag{17}$$

for dilatational transformation. For shear-dilatant transformation, the following form applies to proportional loading:

$$U = \int \tau \, d\gamma_c + \int \sigma_m \, d\varepsilon_m \tag{18}$$

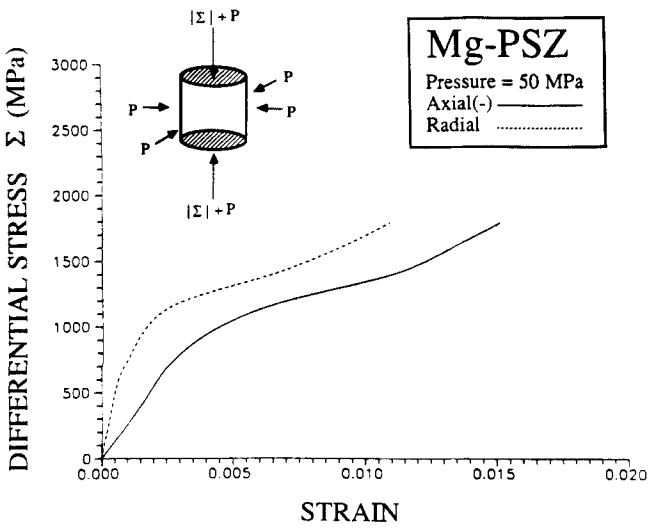

Fig. 3. Stress–strain curves of a Mg-PSZ deformed in uniaxial compression with a superimposed hydrostatic pressure.

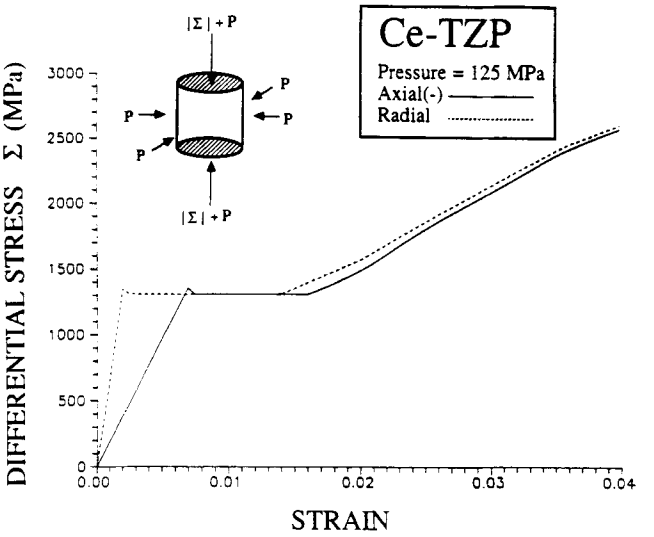

Fig. 4. Stress–strain curves of a Ce-TZP deformed in uniaxial compression with a superimposed hydrostatic pressure.

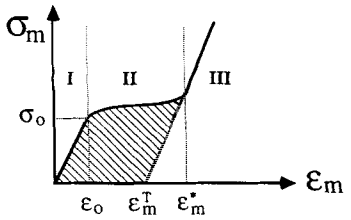

Fig. 5. Schematic stress–strain curve with three stages: the third stage also approximated as linear elastic.

Equation (18) can be reduced, by noting the relations between ε_m and γ_c (Eq. (10)) and between τ, σ_m, and τ_c (Eq. (5)), to a simple form,

$$U = \int \tau_c \, d\gamma_c \tag{19}$$

which is analogous to Eq. (17).

A complete analogy between dilatational transformation and shear-dilatant transformation exists in proportional loading, which can be summarized by the following formal correspondence:

$$\{\sigma_m, \sigma_o, \varepsilon_m^*, \varepsilon_o, \varepsilon_m^T, \omega_m, B\} \leftrightarrow \{\tau_c, \tau_o, \gamma_c^*, \gamma_o, \gamma_c^T, \omega_c, G\} \tag{20}$$

Therefore, the analysis of crack-tip fields and energy dissipation is formally identical for both types of transformation. In the following, we will take advantage of this analogy to write parallel results for dilatational and shear-dilatant transformation.

III. Analysis of Toughening

In steady-state, quasi-static crack growth, a continuous transformation zone of a constant height encircles the crack tip and the fractured surfaces in its wake. The height of the transformation zone is denoted as h_o. Since we also envision a second elastic loading stage following transformation (see III of Fig. 5), there should be a corresponding inner zone within which the transformation strain has saturated. The height of this inner zone is denoted as h_i. The transformation strain in the transitional zone in between is bounded by 0 at h_o and ε_m^T (γ_c^T) at h_i; i.e., the transformation may be partially completed. A schematic illustrating these zones is shown in Fig. 6.

The energy change experienced by a volume element at a height y from the crack plane as it translates from $x = \infty$ to $x = -\infty$ dictates the contribution of the strip dy to the toughness. An energy balance relation for the steady-state crack-growth problem is[5,32]

$$J = J_{tip} + \Delta J = J_{tip} + 2\int_0^{h_o} U(y) \, dy \tag{21}$$

where J is the J-integral, which is a loading parameter driving the crack, and $U(y)$ is the energy dissipation associated with the volume element as it undergoes the loading–unloading cycle. Later, we will let Eqs. (17) to (19) represent $U(y)$ under certain restrictive conditions.

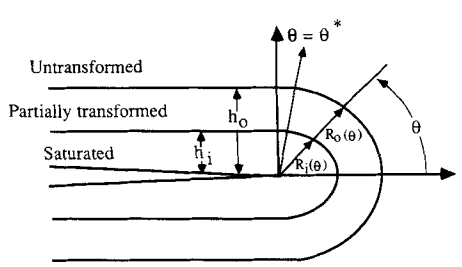

Fig. 6. Crack-tip configuration showing the crack encircled by an inner zone of saturated transformation and an outer transitional zone of partial transformation. The outermost radius r is denoted by R, which coincides with h at $\theta = \theta^*$.

Although a rigorous analysis of toughening requires the solution to the growing crack problem, the approximate method of Evans *et al.*[11] can be adopted to arrive at an approximate solution by appealing to the stationary crack-tip HRR solution.[25–27] The formulation of this solution and its application to $U(y)$, h_o, and h_i is reviewed in the Appendix. More generically, we can simply observe that the strain energy density $U(y)$ is likely to decrease, within an additive constant, inversely with distance y in the range $h_i < y < h_o$, if the stress–strain field is approximately HRR-like. This postulate then allows us to evaluate the integration in Eq. (21) to yield

$$\Delta J = (2n/(n+1))h_o\sigma_o\varepsilon_o \ln (h_o/h_i)$$
$$\Delta J = (2n/(n+1))h_o\tau_o\gamma_o \ln (h_o/h_i) \tag{22}$$

where the logarithmic dependence on h_o/h_i results from the inverse radial distance dependence of U in HRR solutions. This is the toughening contribution due to transformation plasticity.

Equation (22) can be expressed in a more explicit form in terms of materials parameters by noting the following relations from the Appendix:

$$h_i/h_o = (\sigma_o/B\varepsilon_m^*)^{(n+1)/n} \tag{23}$$

$$h_i/h_o = (\tau_o/G\gamma_c^*)^{(n+1)/n} \tag{24}$$

Inserting these relations into Eq. (22), we obtain

$$\Delta J = 2h_o\sigma_o(\sigma_o/B) \ln (B\varepsilon_m^*/\sigma_o)$$
$$= 2h_o\sigma_o(\sigma_o/B) \ln (1 + B\varepsilon_m^T/\sigma_o) \tag{25}$$

$$\Delta J = 2h_o\tau_o(\tau_o/G) \ln (G\gamma_c^*/\tau_o)$$
$$= 2h_o\tau_o(\tau_o/G) \ln (1 + G\gamma_c^T/\tau_o) \tag{26}$$

Note that the second term of the argument of the logarithmic functions is precisely the dimensionless constant ω_m (ω_c) introduced previously.

In the limiting case of weak transformation, Eqs. (25) and (26) can be reduced to the following, by Taylor's expansion of the logarithmic function:

$$\Delta J_o = 2h_o\sigma_o\varepsilon_m^T \tag{27}$$

$$\Delta J_o = 2h_o\tau_o\gamma_c^T \tag{28}$$

where the subscript o is introduced to denote the toughness increment in the weak transformation limit. Equation (27) is the same as that obtained by Budiansky *et al.*[5] for the dilatational transformation using a rigorous energy integration. Equation (28) has been obtained by Chen and Reyes-Morel previously[15] for shear-dilatant transformation.

The logarithmic form of the toughness equations dictates that the toughness increase for strong transformation is not proportional to the strength of transformation, ω_m or ω_c, as for weak transformation. This can be understood by comparing h_o and h_i in the two cases. For weak transformation, Eqs. (23) and (24) show that h_i approaches h_o in the same limit. Thus, the transitional zone vanishes and the transformation is saturated in the entire plastic zone. There is no difference between subcritical and supercritical transformation in this case. (The same point was observed by Budiansky *et al.*[5] in their analysis, as will be discussed later in conjunction with Fig. 7.) On the other hand, for strong transformation, $h_i << h_o$; i.e., a large transitional zone is present. Since the transformation strain in the transitional zone is constrained, by mechanical considerations, to vary almost inversely with r, the resultant toughening contribution is correspondingly smaller.

The above results can be recapitulated succinctly in the following form by rewriting Eqs. (25) and (26) using Eqs. (27) and (28):

$$\Delta J = (\Delta J_o/\omega) \ln (1 + \omega) \tag{29}$$

Here ω is a nondimensional constant denoting ω_m or ω_c, and ΔJ_o is the toughness increment which would be expected, assuming full transformation throughout the zone. In the same notation, the full transformation zone height h_i and the partial transformation zone height h_o are related to each other by

$$h_o/h_i = (1 + \omega)^{(n+1)/n} \approx 1 + \omega \qquad (n >> 1) \tag{30}$$

IV. Stress Intensity Factor and Comparison with Numerical Results

We proceed to estimate the crack-tip stress intensity factor by exploiting the equivalence of J and K in small-scale yielding and compare it with the numerical results in the literature. The relations to be used in this exercise are standard:

$$J = K^2/E' \tag{31}$$

where K is the stress intensity factor, $E' = E$ in plane stress, and $E' = E/(1 - \nu^2)$ in plane strain (E is Young's modulus and ν is Poisson's ratio), and

$$J_{tip} = K_{tip}^2/E' \tag{32}$$

where K_{tip} is designated to be the same as the stress intensity factor without transformation. We also let

$$K = K_{tip} + \Delta K \tag{33}$$

Lastly, by noting the strain equations in the Appendix, we may write

$$h_o = \alpha_m(n, \mu, \omega_m)(K/\sigma_o)^2$$
$$h_o = \alpha_c(n, \mu, \omega_c)(K/\tau_o)^2 \tag{34}$$

where $\alpha_{m,c}$ is taken as a dimensionless constant to be determined later. (Its value may depend on the material constants.) We can then show, by substituting K and K_{tip} for ΔJ in Eqs. (25) and (26) and using Eq. (34) for h_o and Eqs. (15) and (16) for ω_m and ω_c, the following equations:

$$K_{tip}/K = \sqrt{1 - 2\alpha_m(E'/B) \ln (1 + \omega_m)} \tag{35}$$

$$K_{tip}/K = \sqrt{1 - 2\alpha_c(E'/G) \ln (1 + \omega_c)} \tag{36}$$

The interpretation of these results is that the stress intensity at the crack tip is reduced by the transformation, i.e., crack-tip-shielding results.

We postpone the discussion of how α_m and α_c should be evaluated until later. Here, we simply use the result $\alpha_m = 0.077645$, known from the previous work on dilatant transformation,[5] to examine the prediction of Eq. (35). Let $\nu = 0.3$, and note that $B = E/3(1 - 2\nu)$; the ratio K_{tip}/K according to Eq. (35) can be plotted versus ω_m in Fig. 7. For comparison, the results obtained by Amazigo and Budiansky[30] for a supercritically transforming material (i.e., full transformation within h_o), and by Budiansky, Hutchinson, and Lambropoulos[5] for a nonhardening (i.e., $n = \infty$), subcritically transforming material, are also shown. Since the present calculation envisions partial transformation within the transitional zone, it should be compared with the subcritical results of Budiansky, Hutchinson, and Lambropoulos.[5] Throughout the range of ω_m (from 0 to 7), as investigated by Budiansky, Hutchinson, and Lambropoulos, the numerical results, which are rigorous, are in close agreement with ours, which involves approximations in using the stationary crack solution. In comparison, the supercritical results of Amazigo and Budiansky[30] show a much stronger toughening effect at large ω_m because full transformation within h_o is attained in their solution.

We note that all the curves in Fig. 7 show the same initial slope (i.e., in the case of weak transformation). This confirms our previous assertion that the distinction between supercritical and subcritical transformation is irrelevant in this limit because the transitional zone has been squeezed out. In the same limit, Eqs. (35) and (36) reduce to

$$K_{tip}/K = 1 - \alpha_m(E'/B)\omega_m \qquad \Delta K = \varepsilon_m^T E' \sqrt{\alpha_m h_o} \tag{37}$$

$$K_{tip}/K = 1 - \alpha_c(E'/G)\omega_c \qquad \Delta K = \gamma_c^T E' \sqrt{\alpha_c h_o} \tag{38}$$

Equations (37) are identical with the results obtained by Budiansky *et al.*[5] and McMeeking *et al.*[6] for dilatational transformation. Equations (38), for shear-dilatant transformation, are identical with the result obtained by Chen and Reyes-Morel.[15]

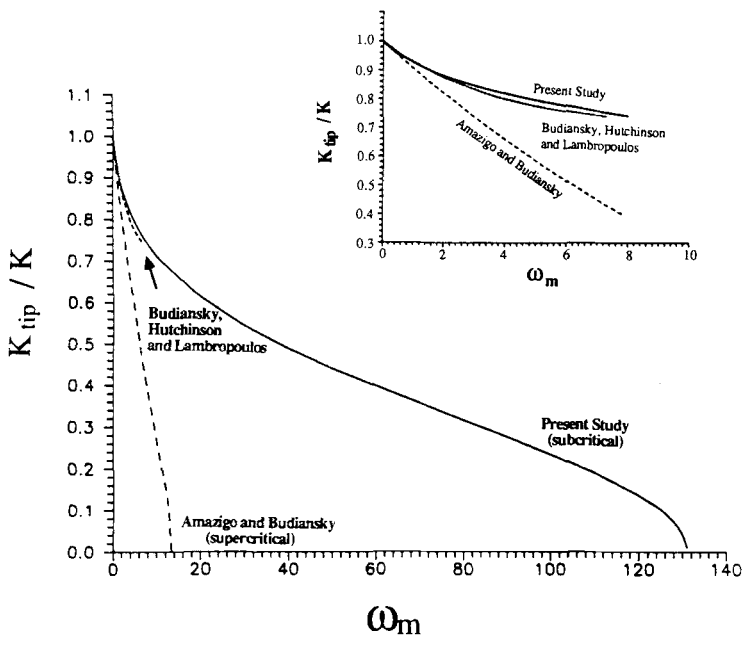

Fig. 7. Ratio of crack-tip shielding, K_{tip}/K, versus the strength of dilatational transformation. Present model prediction appears in close agreement with Budiansky *et al.*[5] finite-element calculation for subcritical transformation. Also shown is the asymptote due to Amazigo and Budiansky[30] for supercritical transformation.

In the other extreme, of strong transformation, the following limiting relations can be shown to hold:

$$\Delta K = \varepsilon_m^T B\sqrt{h_o}/\{\sqrt{\alpha_m}[\exp(B/2\alpha_m E') - 1]\} \quad (39)$$

$$\Delta K = \gamma_c^T G\sqrt{h_o}/\{\sqrt{\alpha_c}[\exp(G/2\alpha_c E') - 1]\} \quad (40)$$

Note that, although the same scaling relation between transformation strain, elastic modulus, $\sqrt{h_o}$, and ΔK still are valid as before, the proportionality constant in Eqs. (39) and (40) is much different. That is, for the same h_o, ΔK is much smaller for strong transformation than that predicted for weak transformation. This point has been experimentally verified.[13,29]

V. Comparison with Experimental Results

(1) Weak Transformation

There is no distinction between models of subcritical and supercritical transformation in this limit because h_o and h_i approach each other. Therefore, the main issue here is the comparison of predictions for dilatational transformation and for shear-dilatant transformation. Since it has been elucidated by several investigators previously,[12,15,33] we will simply recast the results in the present form.

When transformation strains are very small, the crack-tip fields are, to a good approximation, the same as those given by linear elastic solutions. In the case of dilatational transformation, the transformation zone in plane strain is described by

$$r_m = (1/2\pi)[4(1+\nu)^2/9][\cos^2(\theta/2)](K/\sigma_o)^2 \quad (41)$$

and the maximum height of the transformation zone is at $\theta^* = 60°$. Substituting θ^* into $r_m \sin\theta$, and comparing it with Eq. (34), we find

$$\alpha_m = \sqrt{3}(1+\nu)^2/12\pi \quad (42)$$

or 0.077645. Substituting α_m into Eq. (37), we find, in plane strain,

$$\Delta K = [0.2143/(1-\nu)]\varepsilon_m^T E\sqrt{h_o} \quad (43)$$

This is the well-known result first derived by McMeeking and Evans.[6] The same α_m has been used for the computation leading to Fig. 7.

The transformation zone in shear-dilatant transformation is delineated by

$$r = (1/2\pi)\left[\sqrt{\sin^2(\theta/2) + (1-2\nu)^2/3} + 2(1+\nu)\mu/3\right]^2 \times [\cos^2(\theta/2)](K/\tau_o)^2 \quad (44)$$

We have evaluated θ^* and α_c for μ ranging from 0 to 1. These results are plotted in Fig. 8. If we let $\mu = 1/\sqrt{3}$ (representative of Mg-PSZ) and $\nu = 0.3$, we find the maximum height at $\theta^* = 78.6°$ and $\alpha_e = 0.12888$. With the same μ, and noting that $\varepsilon_m^T \approx \mu\gamma_e^T$, we find from Eq. (38) in plane strain that

$$\Delta K = [0.4783/(1-\nu)]\varepsilon_m^T E\sqrt{h_o} \quad (45)$$

These results have been previously obtained by Chen and Reyes-Morel[15] by evaluating the energy integral, assuming full transformation and no hardening.

Equation (45) predicts a stronger toughening effect than does Eq. (43) because both shear and dilatational dissipations have been taken into account. This can also be appreciated by noting that the shear-dilatant transformation zone is much larger than the dilatational transformation zone, for the same reference yield stresses.[12] To the extent that the material constants (μ and ν) are correct, the prediction should be valid in the limit of weak transformation. Data of toughness enhancement in zirconia ceramics have been compiled by Evans and Cannon[33] and are replotted in Fig. 9. The two predictions given by Eqs. (43) and (45) are shown as the upper and lower straight lines, respectively. The shear-dilatant model gives a more satisfactory prediction.

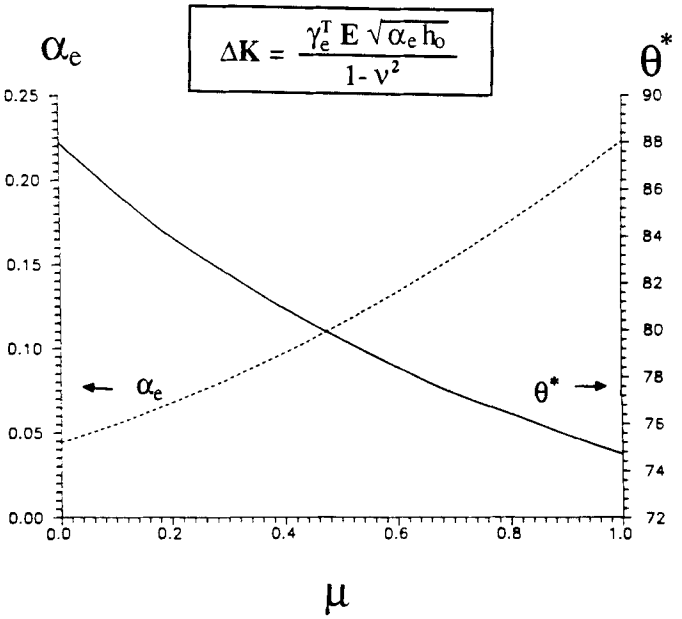

Fig. 8. θ^* and α_c in the weak transformation limit versus μ in the shear-dilatant model.

The limiting case of shear transformation is also delineated in Fig. 8 at $\mu = 0$. It gives $\theta^* = 88°$ for $\nu = 0.3$; hence,

$$\alpha_c \approx [1 + 2(1-2\nu)^2/3]/8\pi \quad (46)$$

or 0.044031, which is well-known in fracture mechanics. Substituting α_e into Eq. (38), we find, in plane strain,

$$\Delta K = [0.1614/(1-\nu)]\gamma_c^T E\sqrt{h_o} \quad (47)$$

(2) Strong Transformation in Ce-TZP

Yu and Shetty[29] have reported, for a Ce-TZP, the following data: $\sigma_o = 183.8$ MPa, $\tau_o = 170.8$ MPa, $\varepsilon_m^T = 0.04$, and $K = 14.5$ MPa·m$^{1/2}$ at $h_o = 0.34$ mm. From these data, we obtain $\mu = 0.929$ and $\gamma_c^T = 0.0431$. Other material parameters appropriate for Ce-TZP, taken from the literature, are $E = 200$ GPa, $\nu = 0.3$, and $K_{tip} = 4$ MPa·m$^{1/2}$. These data give $\omega_c = 19.4$, indicating a case of strong transformation. Substituting the above data into Eq. (26), we find that $\Delta J =$

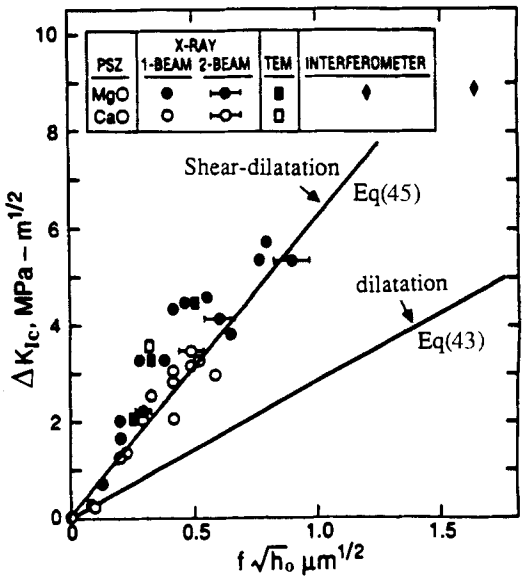

Fig. 9. Toughness data compiled by Evans and Cannon[33] compared with predictions of the shear-dilatant model and dilatational model. f is the fraction of transformation in the McMeeking–Evans model.

7.77×10^{-4} MPa·m. This compares with $J_{tip} = 7.28 \times 10^{-5}$ MPa·m, representing about a 10-fold increase in fracture energy. The computed stress intensity factor is $K = 13.7$ MPa·$m^{1/2}$, which is in reasonable agreement with the reported data. As a check of self-consistency, we infer from Eq. (35) that $\alpha_c = 0.056$ (with the values of $K_{tip}\omega_c$, K, and K_{tip} given above) and compare it directly with the zone size versus K relationship of the form given by Eq. (34) as reported by Yu and Shetty (Fig. 6 of their paper),[29] which gives $\alpha_c = 0.060$. The agreement is satisfactory.

Several investigators have found that the prediction of the weak-transformation model, Eqs. (43) and (45), using the zone height data, overestimates ΔK by a factor of 2 to 6 for Ce-TZP.[13,29] This is understandable if we recall that, for very large values of ω_c, the dependence of toughness on $\sqrt{h_o}$ is much weaker than the weak-transformation model would predict (compare Eqs. (39) and (40) and Eqs. (37) and (38)).

(3) Strong Transformation in Mg-PSZ

Marshall *et al.*[8] have measured the amount of transformation near the crack tip of a Mg-PSZ, which has been aged to a very high toughness, $K = 16$ MPa·$m^{1/2}$. The measured profile of transformation resembles closely that expected from the present analysis. Specifically, the fraction of the monoclinic phase determined by Raman spectroscopy appears to decrease from the crack tip, in a manner which is consistent with the $1/r$ relationship, to an outer zone height of $h_o = 0.9$ mm (see Fig. 4(b) of Marshall *et al.*[8]). Very near the crack tip, the amount of transformation becomes saturated, over a height of $h_i = 0.07$ mm (estimated from the same figure). The saturation fraction of the monoclinic phase is about 25%, giving an estimated saturation strain of $\varepsilon_m^T = 0.01$. Since Marshall *et al.*[8] did not report the data on the yield stress and pressure sensitivity for their material, we take μ to be $1\sqrt{3}$ and n to be 10 as an estimate representative of Mg-PSZ to obtain a tentative assessment of the toughness. Using $G = E/2(1 + \nu) = 76.9$ GPa, $\gamma_c^T \approx \varepsilon_m^T/\mu = 0.0173$, and $h_o/h_i = 13$, we estimate from Eq. (24) that $G\gamma_c^*/\tau_o = 10.3$, or $\omega_c = 9.3$. Thus, this material is also in the strong transformation limit. From these values and Eq. (16), τ_o is estimated to be 143 MPa. Using Eq. (26), we obtain $\Delta J = 1.12 \times 10^{-3}$ MPa·m. This compares with $K_{tip} = 4$ MPa·$m^{1/2}$, or $J_{tip} = 7.28 \times 10^{-5}$ MPa·m, and represents a 15-fold increase of fracture energy. The estimated toughness is $K = 16.2$ MPa·$m^{1/2}$, in good agreement with the reported value for the material. Further confirmation of the above estimation awaits experimental determination of the yield stress and the pressure sensitivity.

VI. Discussion

(1) Crack-Growth Problem

The use of the HRR field of a stationary crack tip for approximate toughness analysis for a growing crack is motivated by mathematical expedience. Evans and co-workers[11] have used essentially the same method to model toughening in rubber-toughened polymers. More recently, Argon[24] has performed a similar analysis for evaluating the toughness contribution due to shear yielding in brittle thermosets. In doing so, however, uncertainties are introduced to model predictions which are difficult to assess a priori. Therefore, the objective of the present effort is less to make definitive claims but more to assess the qualitative trend of various contributions to toughness enhancement under limiting cases. We have been encouraged to do so because the results we obtained have an exceptionally simple form, and, more importantly, in cases where comparisons with rigorous analyses can be made, the agreement is quite good. The comparisons with experimental results of the strong transformation type are also encouraging. In the following paragraphs we make several further observations to explore the implications of these approximations.

Note that, although the present analysis utilizes the HRR field, which is based on the concept of J-integral,[35] the latter cannot lead to any toughness increment, as already discussed by Budiansky, Hutchinson, and Lambropoulos.[5] ($\Delta J = 0$ in Eq. (21) if the J-integral is path independent.) The toughness increment is due to the wake effect, and the HRR field is merely used to make an approximate evaluation of this effect through the integration of dissipation energy $U(y)$.

The stress–strain fields of a growing crack in dilatational, subcritically transforming materials are known from the finite-element calculations of Budiansky *et al.*[5] When the transformation stress is a constant (equal to σ_o), they have graphically illustrated these fields for the nonhardening case, $n = \infty$. In the region between h_i and h_o, the strain varies almost inversely with r from a maximum of ε_m^* at h_i. (The strain is a constant within h_i.) When the strain is normalized by σ_o/B and the distance by JB/σ_o^2, an almost universal strain–distance curve, truncated above by the normalized limiting strain (ω_m), results. These features are all in accord with the expectation for the HRR fields in the nonhardening case. Similar features of strains (i.e., saturation and inverse distance variation) have been observed experimentally by Marshall *et al.*[8] in front of a growing crack, as noted in Section V*(3)*. Therefore, we may tentatively conclude that the HRR field passes for a tolerable solution to the growing-crack problem, at least for dilatational transformation.

For the more general shear-dilatant case, no rigorous growing crack solution is available for comparison and the applicability of the HRR field is uncertain. A further complication for toughness analysis arises because of nonproportional loading around a growing crack, which renders Eq. (18) inexact for the integration of the hysteresis loop when both shear and dilatational contributions are present. Despite these complexities, we expect that the strain fields of a growing crack will bear some resemblance to the HRR field. In particular, the product of stress and strain, or the dissipation energy density $U(y)$, will approximately decrease inversely with distance from $y = h_i$ to $y = h_o$. On this basis, we would expect a similar tendency of a less than linear dependence of the toughness on transformation strain, not unlike the logarithmic form of Eq. (34). Further investigations will be required to verify this expectation.

(2) Constitutive Behavior

There are several features in the constitutive behavior which are central to the present model. First, we have assumed that the fully transformed material returns to the same linear elastic behavior as before. Although this assumption has also been made by essentially all the other investigators in this field, the stress–strain curves shown in Figs. 3 and 4 seem to suggest a reduced modulus after transformation. For such a case, the model can be modified by using the reduced modulus in Eq. (32) for J_{tip}, as first shown by Budiansky, Hutchinson, and Lambropoulos.[5] Second, we have assumed a Mohr–Coulomb type of yield for shear-dilatant transformation. However, the available experimental evidence for the above model is from triaxial compression and uniaxial tension tests, and we have no information whether or not the Mohr–Coulomb yield surface shown in Figs. 1 and 2 is correct at the point of $\tau = 0$. The latter corresponds to hydrostatic tension which actually prevails at the crack tip. (Indeed, the Mohr–Coulomb yield surface has a corner at this point.) Unfortunately, it seems highly unlikely that the state of near hydrostatic tension can be experimentally realized for the purpose of studying constitutive behavior. Therefore, this issue may remain unresolved for some time and further theoretical studies are required to examine the consequence of it in the context of crack-tip fields and transformation toughening.

Other alternative discussions of the toughening due to a shear component of transformation are next discussed and compared with the present work. In the paper of Lambropoulos,[7] several models were treated to assign the shear component of transformation strains of an inclusion.

None of these models, unfortunately, proved capable of predicting the experimentally observed yield surface shown in Figs. 1 and 2 for zirconia. Parallel work was also performed by Seyler, Lee, and Burns,[37] and by Rose,[10] both using dislocation mechanics, to evaluate the stress-shielding effect due to dilatation and shear. These mathematically correct methods nevertheless suffer from their inability to specify the transformation strain field at the crack tip from the available data on constitutive behavior. Instead, all of the above authors have chosen to adopt a certain principal direction for the shear strain which is not generally the same as the principal direction for the shear stress. In this regard, they are essentially assuming a material behavior which disobeys the normality rule in the sense of classical plasticity.[16-18] Since the limited experimental observations of the constitutive behavior of zirconia are in support of the normality rule, we would argue that these calculations are unrealistic regarding the shear behavior.

A rather different approach has been proposed by Rose and Swain,[38] who assume a cohesive zone model for the crack tip, letting the crack propagate when a critical stress is reached over a certain length. This model has been applied to Ce-TZP.[38] In plane stress, the above model is equivalent to the shear-control yield criterion. However, no justification of the above model in plane strain application has thus been provided. Another ad hoc model assumes a certain shape of transformation zone.[33] According to Evans and Cannon,[33] a zone defined by a shear band mode can account for the shear effect even though the transformation strain is only dilatational. Once again, such a model does not satisfy the normality rule.

In the interim, although our model is approximate and strictly applicable only for the idealized material that yields according to the Mohr–Coulomb criterion, it does provide a self-consistent estimate of the shear dilatational strain fields and the stress field in accordance to the yield criterion. It is hoped that the basic predictions of the model will prove to be essentially correct, although they must be regarded as tentative until scrutinized by future investigators.

VII. Conclusions

(1) An approximate method, using Hutchinson–Rice–Rosengren (HRR) asymptotic crack-tip stress–strain fields of a stationary crack to evaluate toughness increments during crack growth, has been applied to modeling transformation toughening.

(2) The increase in steady-state toughening is estimated to be $\Delta J = (\Delta J_0/\omega) \ln (1 + \omega)$, where ΔJ_0 denotes the toughness increment expected for assuming full transformation throughout the zone, and ω is a nondimensional parameter giving the ratio of transformation strain to yield strain.

(3) For dilatational transformation, our results are in good agreement with those of previous investigators using a variety of rigorous methods. It extends the earlier result of McMeeking and Evans[6] which is restricted to weak transformation, $\omega << 1$.

(4) The transformation strain may include a shear component. In the limit of weak transformation, the inclusion of shear transformation is predicted to provide more toughness. Based on the available data on constitutive behavior, the predicted total toughening for shear-dilatant transformation appears in good agreement with the data compiled by Evans and Cannon.[33]

(5) In the limit of strong transformation, a rapidly decreasing toughening efficiency is due to the rapidly decreasing amount of transformation plasticity at an increasing distance from the crack tip. The height of the inner zone, h_i, within which transformation has proceeded to completion (saturation) is essentially $h_0/(1 + \omega)$, where h_0 is the outer zone height. A tentative comparison with experimental observations finds good agreement between the predicted and the measured toughness for Ce-TZP and Mg-PSZ.

APPENDIX

The HRR Solution

Although a rigorous analysis of toughening requires the solution to the growing-crack problem, we will adopt the approximate method of Evans *et al.*[11] to arrive at an estimate by appealing to the stationary crack Hutchinson–Rice–Rosengren (HRR) solution.[25-27] The asymptotic stress and strain fields near a stationary crack tip can be written as[19]

$$\sigma_m(r,\theta) = \sigma_0(J/\sigma_0\varepsilon_0 Ir)^{1/(n+1)}\tilde{\sigma}_m(\theta) \tag{A-1}$$

$$\varepsilon_m(r,\theta) = \varepsilon_0(J/\sigma_0\varepsilon_0 Ir)^{n/(n+1)}\tilde{\varepsilon}_m(\theta) \tag{A-2}$$

where (r,θ) are the polar coordinates with respect to the crack tip and J is the so-called J-integral.[35] The dimensionless constant I and dimensionless angular functions $\tilde{\sigma}_m(\theta)$ and $\varepsilon_m(\theta)$ are dependent on the material constants (n and μ). The determination of I and the two angular functions of stress and strain amplitudes are not central to the present paper. However, we may note the following relation by using Eq. (2):

$$\tilde{\varepsilon}_m(\theta) = \tilde{\sigma}_m^n(\theta) \tag{A-3}$$

The same considerations lead to the following stress and strain fields in the case of shear-dilatant plasticity:

$$\tau_e(r,\theta) = \tau_0(J/\tau_0\gamma_0 Ir)^{1/(n+1)}\tilde{\tau}_e(\theta) \tag{A-4}$$

$$\gamma_e(r,\theta) = \gamma_0(J/\tau_0\gamma_0 Ir)^{n/(n+1)}\tilde{\gamma}_e(\theta) \tag{A-5}$$

The dilatational strain, not given here, is related to γ_e by Eq. (10). In Eqs. (A-4) and (A-5), I, $\tilde{\tau}_e(\theta)$, and $\tilde{\gamma}_e(\theta)$ are again a dimensionless constant, and angular functions, respectively, whose values are dependent on the material constants. Similarly, the following relation is obeyed by virtue of Eq. (7):

$$\tilde{\gamma}_e(\theta) = \tilde{\tau}_e^n(\theta) \tag{A-6}$$

Similar stress and strain fields were used by Evans *et al.*[11] to estimate the toughening contributions of rubber dilatation in the crack tip in polymers. Note that, for large n, corresponding to low strain hardening, the strain field decays from the crack tip in almost a $1/r$ manner. Thus, the existence of a region of partial transformation is a natural consequence of the crack-tip mechanics for a stationary crack.

The above stress and strain fields may be used in conjunction with Eqs. (17), (18), or (19) to evaluate $U(y)$ in a proportional loading–unloading path near a stationary crack tip. Specifically, we focus a volume element lying along $\theta = \theta^*$ in Fig. 6 between the tip of a stationary crack and the highest edge of the frontal zone. This is chosen because, if the stress and strain fields of a stationary crack were to approximate those of a growing crack well, then the maximum loading would occur when a material element passes $\theta = \theta^*$. Integration of U using Eqs. (17) and (19) yields a simple form since the stress and strain are related to each other by the power law. For $h_i < y < h_0$,

$$U = [n/(n + 1)](\sigma_m\varepsilon_m - \sigma_0\varepsilon_0)$$

$$U = [n/(n + 1)](\tau_e\gamma_e - \tau_0\gamma_0) \tag{A-7}$$

In Eq. (A-7), the second factor comes from the exclusion of (nonlinear) elastic loading from dissipation energy; i.e., $U = 0$ when $\varepsilon_m = \varepsilon_0(\gamma_e = \gamma_0)$. For $h_0 < y$, i.e., outside the transformation zone, the integration vanishes. For $y < h_i$, U is a constant:

$$U = [n/(n + 1)](\sigma_m^*\varepsilon_m^* - \sigma_0\varepsilon_0)$$

$$U = [n/(n + 1)](\tau_e^*\gamma_e^* - \tau_0\gamma_0) \tag{A-8}$$

where $\sigma_m^*(\tau_e^*)$ is the stress at $\varepsilon_m = \varepsilon_m^*(\gamma_e = \gamma_e^*)$ in the stress–strain curve. Equation (A-8) corresponds to the maximum

dissipation illustrated by the shaded area in Fig. 5. Note that U varies, within an additive constant $\sigma_0\varepsilon_0(\tau_0\gamma_0)$, inversely with the radial distance from the crack tip, if the HRR singularity solutions are used to evaluate stress and strain.

The following relations for the zone height also follow from the strain expressions, Eqs. (A–2) and (A–5):

$$h_i(\theta) = h_o(\theta)(\sigma_o/B\varepsilon_m^*)^{(n+1)/n} \quad \text{(A–9)}$$

$$h_i(\theta) = h_o(\theta)(\tau_o/G\gamma_e^*)^{(n+1)/n} \quad \text{(A–10)}$$

In Eqs. (A–9) and (A–10), Eqs. (A–3) and (A–6) were used to eliminate the angular functions in Eqs. (A–2) and (A–5).

Acknowledgment: The calculations and graphic art of Mr. S-Y.W. Liu are greatly appreciated.

References

[1]R. C. Garvie, R. H. Hannink, and R.T. Pascoe, "Ceramic Steel?," *Nature (London)*, **258** [5537] 703–704 (1975).

[2]N. Claussen, "Fracture Toughness of Al_2O_3 with an Unstabilized ZrO_2 Dispersed Phase," *J. Am. Ceram. Soc.*, **59** [1–2] 49–51 (1976).

[3]K. Tsukuma and M. Shimada, "Strength, Fracture Toughness, and Vickers Hardness of ZrO_2-Stabilized Tetragonal ZrO_2 Polycrystals (Ce-TZP)," *J. Mater. Sci.*, **204** [4] 1178–84 (1985).

[4]W. M. Kriven, W. L. Fraser, and S.W. Kennedy, "The Martensite Crystallography of Tetragonal Zirconia"; pp. 82–97 in Advances in Ceramics, Vol. 3, *Science and Technology of Zirconia*. Edited by A. H. Heuer and L.W. Hobbs. American Ceramic Society, Columbus, OH, 1981.

[5]B. Budiansky, J.W. Hutchinson, and J.C. Lambropoulos, "Continuum Theory of Dilatant Transformation Toughening in Ceramics," *Int. J. Solids Struct.*, **19** [4] 337–55 (1983).

[6]R. McMeeking and A. G. Evans, "Mechanisms of Transformation Toughening in Brittle Materials," *J. Am. Ceram. Soc.*, **65** [5] 242–45 (1982).

[7]J. C. Lambropoulos, "Shear, Shape, and Orientation Effects in Transformation Toughening," *Int. J. Solids Struct.*, **22** [10] 1083–106 (1986).

[8]D. B. Marshall, M. C. Shaw, R. H. Dauskardt, R. O. Ritchie, M. Ready, and A. H. Heuer, "Crack-Tip Transformation Zones in Toughened Zirconia," *J. Am. Ceram. Soc.*, **73** [9] 2659–66 (1990).

[9]D. B. Marshall, A. G. Evans, and M. Drory, "Transformation Toughening in Ceramics"; pp. 309–26 in *Fracture Mechanics of Ceramics*, Vol. 6. Edited by R. C. Bradt, A. G. Evans, and F. F. Lange. Plenum Press, New York, 1983.

[10]L. R. F. Rose, "The Mechanics of Transformation Toughening," *Proc. R. Soc. London A.* **412**, 151 (1987).

[11]A. G. Evans, Z. B. Ahmad, D. G. Gilbert, and P.W. R. Beaumont, "Mechanisms of Toughening in Rubber-Toughened Polymers," *Acta Metall.*, **34** [1] 79–87 (1986).

[12]I-W. Chen and P. E. Reyes-Morel, "Implications of Transformation Plasticity in ZrO_2-Containing Ceramics: I, Shear and Dilatation Effects," *J. Am. Ceram. Soc.*, **69** [3] 181–89 (1986).

[13]P. E. Reyes-Morel and I-W. Chen, "Transformation Plasticity of CeO_2-Stabilized Tetragonal Zirconia Polycrystals: Stress Assistance and Autocatalysis," *J. Am. Ceram. Soc.*, **71** [6] 343–53 (1988).

[14]P. E. Reyes-Morel, J-S. Cherng, and I-W. Chen, "Transformation Plasticity of CeO_2-Stabilized Tetragonal Zirconia Polycrystals: II, Pseudoelasticity and Shape Memory Effect," *J. Am. Ceram. Soc.*, **71** [8] 648–57 (1988).

[15]I-W. Chen and P. E. Reyes-Morel, "Transformation Plasticity and Transformation Toughening in Mg-PSZ and Ce-TZP"; pp. 75–88 in *Advanced Structural Ceramics*. Edited by P. F. Becher, M.V. Swain, and S. Sōmiya. Materials Research Society, Pittsburgh, PA, 1986.

[16]D. C. Drucker, "Plasticity Theory, Strength-Differential Phenomenon, and Volume Expansion in Metals and Plastics," *Metall. Trans.*, **4**, 667–73 (1973).

[17]J.W. Rudnicki and J. R. Rice, "Plane Strain Deformation Near a Crack Tip in a Pressure-Sensitive Dilatant Material," *J. Mech. Phys. Solids*, **23**, 371–94 (1975).

[18]A. Needleman and J. R. Rice, "Limits to Ductility Set by Plastic Flow Localization"; pp. 237–67 in *Mechanics of Sheet-Metal Forming*. Edited by D. P. Koistinen and Neng-Ming Wang. Plenum, New York, 1978.

[19]F. Z. Li and J. Pan, "Plane-Strain Crack-Tip Fields for Pressure-Sensitive Dilatant Materials," *ASME J. Appl. Mech.*, **57**, 40–49 (1990).

[20]F. A. McClintock and G. R. Irwin, "Plasticity Aspects of Fractive Mechanics," *ASTM Spec. Tech. Publ.*, **381**, 84–113 (1965).

[21]A. D. Chitaley and F. A. McClintock, "Elastic-Plastic Mechanisms of Steady Crack Growth under Anti-Plane Shear," *J. Mech. Phys. Solids*, **19**, 147–63 (1971).

[22]J. R. Rice and E. P. Sorensen, "Continuing Crack-Tip Deformation and Fracture for Plane-Strain Crack Growth in Elastic-Plastic Solids," *J. Mech. Phys. Solids*, **26**, 163–86 (1978).

[23]J. R. Rice, W. J. Drugan, and T-L. Sham, "Elastic-Plastic Analysis of Growing Cracks," *ASTM Spec. Tech. Publ.*, **700**, 189–221 (1980).

[24]W. J. Drugan, J. R. Rice, and T-L. Sham, "Asymptotic Analysis of Growing Plane Strain Tensile Cracks in Elastic-Ideally Plastic Solids," *J. Mech. Phys. Solids*, **30**, 447–73 (1982).

[25]J.W. Hutchinson, "Singular Behavior at the End of a Tensile Crack in a Hardening Material," *J. Mech. Phys. Solids*, **16**, 13–32 (1968).

[26]J.W. Hutchinson, "Plastic Stress and Strain Fields at a Crack Tip," *J. Mech. Phys. Solids*, **16**, 337–47 (1968).

[27]J. R. Rice and G. F. Rosengren, "Plane Strain Deformation Near a Crack Tip in a Power-Law Hardening Material," *J. Mech. Phys. Solids*, **16**, 1–12 (1968).

[28]J. Pan and I-W. Chen; unpublished work.

[29]C. S. Yu and D. K. Shetty, "Transformation Zone Shape, Size, and Crack-Growth-Resistance (*R*-Curve) Behavior of Ceria-Partially-Stabilized Zirconia Polycrystals," *J. Am. Ceram. Soc.*, **72** [6] 921–28 (1989).

[30]J. C. Amazigo and B. Budiansky, "Steady-State Crack Growth in Supercritically Transforming Materials," *Int. J. Solids Struct.*, **24**, 751-55 (1988).

[31]P. E. Reyes-Morel, "An Experimental Study of Constitutive Relations of Transformation Plasticity in Zirconia-Based Ceramics"; Ph. D. Thesis. Department of Nuclear Engineering, Massachusetts Institute of Technology, Cambridge, MA, June 1986.

[32]J.W. Hutchinson, "On Steady Quasi-Static Crack Growth," Harvard University Report, Division of Applied Science, DEAP S-8. Harvard University Press, Cambridge, MA, 1974.

[33]A. G. Evans and R. M. Cannon, "Toughening of Brittle Solids by Martensitic Transformations," *Acta Metall.*, **34**, 761–800 (1986).

[34]A. S. Argon, "Sources of Toughness in Polymers"; pp. 2661–81 in *7th International Conference on Fracture*, Vol. 4. Pergamon Press, New York, 1989.

[35]J. R. Rice, "A Path-Independent Integral and the Approximate Analysis of Strain Concentration by Notches and Cracks," *ASME J. Appl. Mech.*, **35** [6] 379–86 (1968).

[36]J. C. Amazigo and B. Budiansky, "Crack-Tip Fields in Steady Crack-Growth with Linear Strain-Hardening," *J. Mech. Phys. Solids*, **25**, 81–91 (1977).

[37]R. J. Seyler, S. Lee, and S. J. Burns, "A Thermodynamic Approach to Fracture Toughness in PSZ"; pp. 213–24 in Advances in Ceramics, Vol. 12, *Science and Technology of Zirconia II*. Edited by N. Claussen, M. Rühle, and A. H. Heuer. American Ceramic Society, Columbus, OH, 1984.

[38]L. R. F. Rose and M.V. Swain, "Transformation Zone Shape in Ceria-Partially Stabilized Zirconia," *Acta Metall.*, **36**, 955–62 (1988). □